J Inorg Organomet Polym
DOI 10.1007/s10904-017-0569-x

Synthesis, Characterization and Biological Activity of New 3-substitued-4-amino-5-hydrazino-1,2,4-triazole Schiff Bases and Their Cu(II) Complexes: A New Approach to CuO Nanoparticles for Photocatalytic Degradation of Methylene Blue Dye

Mostafa Y. Nassar[1] · Hisham M. Aly[1] · Moustafa E. Moustafa[1] · Ehab A. Abdelrahman[1]

Received: 25 February 2017 / Accepted: 2 May 2017

Abstract Three new Schiff base compounds were synthesized via condensation of 3-R-4-amino-5-hydrazino-1,2,4-triazole with dibenzoylmethane [R = H, CH_3, and CH_2CH_3 namely L1, L2, and L3, respectively]. The synthesized Schiff bases were characterized using melting point, CHN elemental analyses, FT-IR, and ^{1}H-NMR. The corresponding Cu(II) Schiff base complexes were synthesized via refluxing the prepared Schiff bases with $CuCl_2{\cdot}2H_2O$. The synthesized complexes have been characterized by means of different spectral tools (FT-IR, ESR, and UV–Vis spectra) in addition to elemental analysis, magnetic moment, conductivity, and thermal analysis. The synthesized copper complexes are nonelectrolytes in *N,N*-dimethylformamide (DMF) based on their conductance values. Using modified Bauer-Kirby method, the Schiff bases and their Cu(II) complexes have been tested for antifungal (*Candida albicans* and *Aspergillus flavus*) and antibacterial (*Staphylococcus aureus* and *Escherichia coli*) activities. Moreover, CuO nanoparticles were produced via thermal decomposition of the synthesized Cu(II) complexes at 650 °C. The produced nanoparticles were characterized using XRD, HR-TEM, FT-IR, and UV–Vis spectroscopy. The CuO nanostructures exhibited good photocatalytic activity for the degradation of methylene blue dye in the presence of hydrogen peroxide with 77.36% degradation efficiency in 360 min.

Graphical Abstract Proposed structure of the synthesized Cu(II) complexes

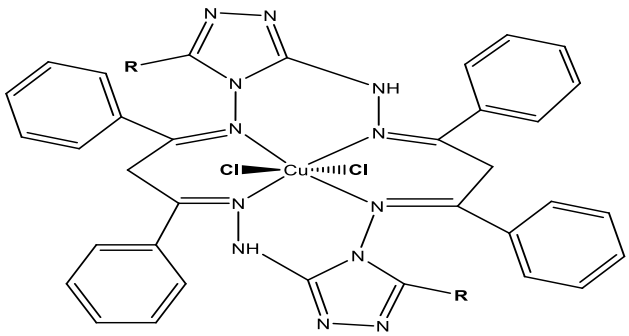

Keywords Cu(II)-Schiff base complexes · Biological activity · CuO nanoparticles · Methylene blue · Photocatalytic degradation

1 Introduction

Compounds containing 1,2,4-triazole derivatives possess several applicable properties in many fields such as industrial and biological areas [1–4]. Quite recently, a considerable attention of many researchers has been paid to the preparation of 1,2,4-triazole Schiff base compounds for using them as antioxidant, antitumor and antimicrobial agents [5–8]. The published results have shown that these compounds possess effective role against bacteria and fungi which may be due to hetero atoms and/or azomethine linkage present in these compounds. Recently, scientists are interested in production of new 1,2,4-triazole Schiff base complexes with different

✉ Mostafa Y. Nassar
m_y_nassar@yahoo.com; m_y_nassar@fsc.bu.eg.edu

[1] Chemistry Department, Faculty of Science, Benha University, Benha 13518, Egypt

Published online: 12 May 2017

metal ions because the biological efficiencies of the ligands increases as a result of the metal–ligand linkage as explained by Overton's concept and chelation theory. Moreover, metal ion complexes of Schiff bases have two important criteria: the first is their excellent biological effect, and the second is the ability to produce metal oxide nanoparticles as cheap and inexpensive method for the production of nanoparticles with novel structures and good purity [9]. Among nano-sized metal oxides, CuO still play an important role because of their vast applications in quenchometric determination of atorvastatin, rivastigmine and topiramate [10], sensor applications [11], enhanced lithium storage performance [12], and photocatalytic degradation of dyes from aqueous solutions [13, 14]. Although there are numerous valid methods for synthesis of copper oxide nanostructures such as microwave-assisted template-free, hydrothermal, and others, these methods are require long time and/or complicated [15–18]. Using coordination Cu(II) complexes as precursors for the synthesis of copper oxide nanoparticles has been considered as one of the greatest convenient and excellent practical approaches [9]. The present work focuses on the synthesis and biological evaluation of some new triazole Schiff bases and their Cu(II) complexes. As such the triazole Schiff bases are produced by reacting of 3-substitued-4-amino-5-hydrazino-1,2,4-triazole and dibenzoylmethane. The synthesized Schiff bases were characterized using melting point, CHN elemental analysis, FT-IR, and ^{1}H-NMR whereas their Cu(II) complexes have been characterized by means of spectral tools (FT-IR, ESR, and UV–Vis spectra) in addition to elemental analysis, magnetic moment, conductivity, and thermal analysis. Moreover, copper oxide nanoparticles have been generated by thermal decomposition of the synthesized 3-substitued-4-amino-5-hydrazino-1,2,4-triazole Schiff base-copper(II) complexes. The produced oxide was also examined for the photocatalytic degradation of methylene blue dye aqueous solution in the presence of hydrogen peroxide under UV illumination. The produced copper oxides were characterized using XRD, HR-TEM, FT-IR, and UV–Vis spectra.

2 Experimental

2.1 Materials and Reagents

Dibenzoylmethane and copper chloride dihydrate were obtained from Aldrich chemical company. All solvents were of analytical reagent grade and used as received without further purification. The thiocarbohydrazide and 3-substituted-4-amino-5-hydrazino-1,2,4-triazoles were prepared as reported [19, 20].

2.2 Synthesis of Precursors

2.2.1 Synthesis of Triazole Schiff Bases

A methanolic solution of dibenzoylmethane was mixed with a methanolic solution of the synthesized 3-R-4-amino-5-hydrazino-1,2,4-triazole (R = H, CH_3 or C_2H_5) in a 1:1 molar ratio. Afterward, the reaction mixture was acidified by addition of few drops of concentrated H_2SO_4. Then, the reaction blend was refluxed with continuous stirring for about 5 h. Thence, the reaction mixture was left for some time to acquire the room temperature. The produced yellow precipitate was filtered off, washed with cold ether and methanol, re-crystallized from ethanol, and vacuum dried. The prepared Schiff bases are referred to as **L1, L2** and **L3**, and the percent yields are 68.5, 77.5 and 75.5% yield, respectively. *Anal.Calc*. In case of **L1**, $C_{34}H_{32}N_{12}O_2$, m.p. = 92–93 °C, MW = 640.28: C, 63.74; H, 5.03; N, 26.23%. Found: C, 63.76; H, 5.09; N, 26.30%. ^{1} H-NMR (DMSO-d_6), δ, ppm: 11.20 (s, 2H, NH), 7.20–8.40 (m, 20H, Ar–H), 4.85 (s, 4H, aliphatic CH_2), 6.33 (s, 2H, H-Triazole). FT-IR, ν, cm^{-1}: 3470 (NH of Triazole ring and adsorbed H_2O molecules, medium broad, stretching vibrations), 1628 (C=N, medium, stretching vibration; H_2O, medium, bending vibration), 1580–1410 (C=C, multi-bands, aromatic stretching vibration), 780–745 (C–H, multi-bands, out of plane bending vibration of aromatic rings).

In case of **L2**, $C_{36}H_{34}N_{12}O$, m.p. = 112–113 °C, MW = 650.30: C, 66.45; H, 5.27; N, 25.83%. Found: C, 66.50; H, 5.30; N, 26.00%. ^{1} H-NMR (DMSO-d_6), δ, ppm: 11.40 (s, 2H, NH), 7.20–8.40 (m, 20H, Ar–H), 4.85 (s, 4H, aliphatic CH_2), 2.40 (s, 6H, CH_3-Triazole). FT-IR, ν, cm^{-1}: 3480 (NH of Triazole ring and adsorbed H_2O molecules, medium broad, stretching vibrations), 1623 (C=N, medium, stretching vibration; H_2O, medium, bending vibration), 1570–1480 (C=C, multi-bands, aromatic stretching vibration), 785–755 (C–H, multi-bands, out of plane bending vibration of aromatic rings).

In case of **L3**, $C_{38}H_{38}N_{12}O$, m.p. = 130–131 °C, MW = 678.32: C, 67.24; H, 5.64; N, 24.76%. Found: C, 67.80; H, 5.92; N, 25.64%. ^{1} H-NMR (DMSO-d_6), δ, ppm: 11.20 (s, 2H, NH), 7.20–8.40 (m, 20H, Ar–H), 4.85 (s, 4H, aliphatic CH_2), 1.19 (t, 6H, CH_3-Triazole), 2.65 (q, 4H, CH_2-Triazole). FT-IR, ν, cm^{-1}: 3500 (NH of Triazole ring and adsorbed H_2O molecules, medium broad, stretching vibrations), 1620 (C=N, medium, stretching vibration; H_2O, medium, bending vibration), 1550–1490 (C=C, multi-bands, aromatic stretching vibration), 785–760 (C–H, multi-bands, out of plane bending vibration of aromatic rings).

2.2.2 Synthesis of Cu(II) Triazole Schiff Base Complexes

An ethanolic solution (25 mL) of the Schiff bases (**L1, L2** or **L3**) (1.0 mmol) was refluxed with 1.0 mmol of copper chloride dihydrate in 25 mL ethanol for 5 h. Then, to the reaction mixture, 2.0 mmol of sodium acetate trihydrate was added, and refluxed was continued for another 5 h. After that, the complexes were separated by filtration, washed thoroughly with ethanol, ether and water, and finally vacuum dried.

Anal.Calc. In case of Cu-**L1**, $C_{34}Cl_2Cu\ H_{32}N_{12}O_2$, MW = 773.14: C, 52.68; H, 4.16; N, 21.68%. Found: C, 52.30; H, 4.11; N, 21.48%. FT-IR, ν, cm^{-1}: 3455 (NH of Triazole ring and adsorbed H_2O molecules, medium broad, stretching vibration), 1605 (C=N, medium, stretching vibration; H_2O, medium, bending vibration), 1579–1408 (C=C, multi-bands, aromatic stretching vibration), 788–746 (C–H, multi-bands, out of plane bending vibration of aromatic rings), 525 (M-N, medium, stretching vibration). In case of Cu-**L2**, $C_{36}Cl_2CuH_{36}N_{12}O_2$, MW = 801.17: C, 53.92; H, 4.49; N, 20.97%. Found: C, 54.00; H, 4.29; N, 21.03%. FT- IR, ν, cm^{-1}: 3455 (NH of Triazole ring and adsorbed H_2O molecules, medium broad, stretching vibration;), 1607 (C=N, medium, stretching vibration; H_2O, medium, bending vibration), 1584–1415 (C=C, multi-bands, aromatic stretching vibration), 780–750 (C–H, multi-bands, out of plane bending vibration of aromatic rings), 525 (M-N, medium, stretching vibration). In case of Cu-**L3**, $C_{38}Cl_2CuH_{42}N_{12}O_4$, MW = 863.21: C, 52.83; H, 4.86; N, 19.46%. Found: C, 52.65; H, 4.70; N, 19.29%. FT-IR, ν, cm^{-1}: 3470 (NH of Triazole ring and adsorbed H_2O molecules, medium broad, stretching vibration), 1599 (C=N, medium, stretching vibration; H_2O, medium, bending vibration), 1579–1416 (C=C, multi-bands, aromatic stretching vibration), 784–747 (C–H, multi-bands, out of plane bending vibration of aromatic rings), 523 (M-N, medium, stretching vibration).

2.3 Synthesis of CuO Nanoparticles

The as-prepared Cu(II)-**L1**, Cu(II)-**L2** and Cu(II)-**L3** triazole Schiff base complexes were thermally decomposed at 650 °C for 2 h in an electrical muffle to give the corresponding CuO nanoparticles.

2.4 Physical Measurements

FT-IR spectra of the triazole Schiff bases, their copper complexes and copper oxides were recorded on a Nicolet iSio FT-IR spectrophotometer in the 4000–400 cm^{-1} region in KBr disks (Chemistry department, Faculty of Science, Benha University, Egypt). Electronic absorption spectra of the copper complexes were recorded in *N,N*-dimethylformamide (DMF) and Nujol oil on Jasco (V-530) UV–Vis spectrophotometer (Chemistry department, Faculty of Science, Benha University, Egypt). The ^{1}H-NMR spectra of triazole Schiff bases were recorded in DMSO on a Bruker 300 MHz spectrometer at room temperature using tetramethyl silane (TMS) as an internal reference (Faculty of Science, Cairo University, Giza, Egypt). Elemental analyses for C, H and N were performed using Elementer Vario EL III Carlo Erba 1108 instrument (The Regional Center for Mycology and Biotechnology, Al-Azhar University, Cairo, Egypt). While molar conductivity measurements of the copper complexes were recorded on an YSI conductivity bridge with a cell having cell constant 1 (Chemistry department, Faculty of Science, Benha University, Egypt). The molar magnetic susceptibility; χ_M, of the synthesized copper complexes was measured using a Gouy balance at room temperature (Faculty of Education, Ain shams University, Egypt). The sample was packed in a Gouy tube of known mass. Mercury(II) tetrathiocyanatocobaltate(II) [$Hg\{Co(SCN)_4\}$] was used for the calibration of the Gouy tube. The obtained values were corrected for diamagnetism using Pascal's constants. Differential thermal and thermogravimetric analysis (DTA-TGA) of the synthesized copper complexes were recorded using Shimadzu TA-60 WS thermal analyzer (Micro analytical unit, Cairo University, Giza, Egypt). Measurement started from room temperature up to 1000 °C using N_2 as an atmosphere at heating rate of 10 °C min^{-1}. ESR spectra of Cu (II) complexes were recorded on Varian E-9 spectrophotometer (Micro analytical unit, Tanta University, Tanta, Egypt). X-ray powder diffraction (XRD) of the product nanostructures were recorded on a 18 kW diffractometer (Bruker; model D8 Advance) with monochromated Cu Kα radiation (λ) 1.54178 Å (Central Metallurgical Research Institute, Cairo, Egypt). The HR-TEM images of copper oxide nanoparticles were taken on a transmission electron microscope (JEOL; model 1200 EX) at an accelerator voltage of 220 kV (Petroleum Research Institute, Cairo, Egypt).

2.5 Biological Activity

Using modified Bauer–Kirby method [9], antimicrobial activities of the synthesized triazole Schiff bases, their Cu(II) complexes, and as-prepared copper oxide nanoparticles were determined. It is noteworthy that 100 µL of the pathogenic fungi/bacteria in 10 mL of fresh media were grown until they reached a count of 105 cells per mL for fungi or 108 cells per mL for bacteria. After that 100 µL microbial suspensions were spread onto agar plates corresponding to the both pathogens in which they were maintained. By disc diffusion method, isolated colonies of each organism were tested for susceptibility. A filter paper disc impregnated with the tested compounds was placed on agar

where plates with fungi (*Candida albicans* and *Aspergillus flavus*) were incubated at 25–27 °C for 24–48 h. and plates with gram positive bacteria (*Staphylococcus aureus*)/ gram negative bacteria (*Escherichia coli*) were incubated at 35–37 °C for 24–48 h. The inhibition zone diameters were measured in millimeters.

2.6 Photocatalytic Degradation

The Photocatalytic degradation of methylene blue dye was investigated using copper oxide products prepared using Cu(II)-**L3** complex. For an ideal photocatalytic experiment, 0.1 g of the prepared copper oxide photocatalyst was added to 50 mL of 10 mg L^{-1} aqueous dye solution. A suspension of CuO nanoparticles and aqueous dye solution was stirred for 2 h in dark to achieve an adsorption–desorption equilibrium. After that, 2 mL of 0.2 M hydrogen peroxide solution was added and the suspension was undergone UV light (at 365 nm) irradiation. The degradation was studied in a Pyrex beaker under the UV illumination using a 250 W xenon arc lamp (Thoshiba, SHLS-002) (λ = 365 nm). After separating the copper oxide catalyst by centrifugation, the absorption of the remaining solution was recorded at 664 nm (λ_{max} for methylene blue dye) at a pre-definite time using a UV–Vis spectrophotometer.

3 Results and Discussion

3.1 Synthesis and Characterization of L1, L2 and L3 Triazole Schiff Bases

The new Schiff bases were synthesized via the condensation of 3-R-4-amino-5-hydrazino-1,2,4-triazole (R = H, CH_3 or C_2H_5) with dibenzoylmethane in a methanolic solution at 1:1 molar ratio under reflux in the presence of few drops of concentrated H_2SO_4. The synthesized Schiff bases were characterized using m.p, FT-IR, ^{1}H-NMR, and CHN elemental analysis. The Practical values of C, H, and N% are in excellent agreement with the proposed molecular formulas (Theoretical values).

3.1.1 FT-IR Spectra of L1, L2 and L3 Triazole Schiff Bases

The FT-IR spectra of the synthesized triazole Schiff bases show different bands (***c.f***. Fig. 1), a medium intensity broad band appeared in the range 3500–3470 cm^{-1} which may be due to NH stretching vibration of the triazole ring and adsorbed water molecules. Whereas, a medium to high intensity band observed in the range 1628–1620 cm^{-1} is probably assigned to stretching C=N and bending H_2O vibrations. Moreover, bands appeared at 3500–3470 and 1628–1620 cm^{-1} can be also assigned to stretching and bending vibrations of the adsorbed surface water molecules [21–27]. Numerous absorptions bands appeared in the region 1570–1400 cm^{-1} are attributed to C=C aromatic stretching vibrations whereas bands in the region of 785–745 cm^{-1} are due to C–H out of plane bending vibration of aromatic rings [28].

3.1.2 ^{1}H-NMR Spectra of L1, L2 and L3 Triazole Schiff Bases

The ^{1}H-NMR spectra (in d_6-DMSO) of the synthesized triazole Schiff bases showed signals at about : 11.20 (s, 2H, NH) (**L1** and **L3**), 11.40 (s, 2H, NH) (**L2**), 7.20–8.40 (m, 20H, Ar–H), 4.85 (s, 4H, aliphatic CH_2), 6.33 (s, 2H, H-Triazole-**L1**), 2.40 (s, 6H, CH_3-Triazole-**L2**), 1.19 (t, 6H,

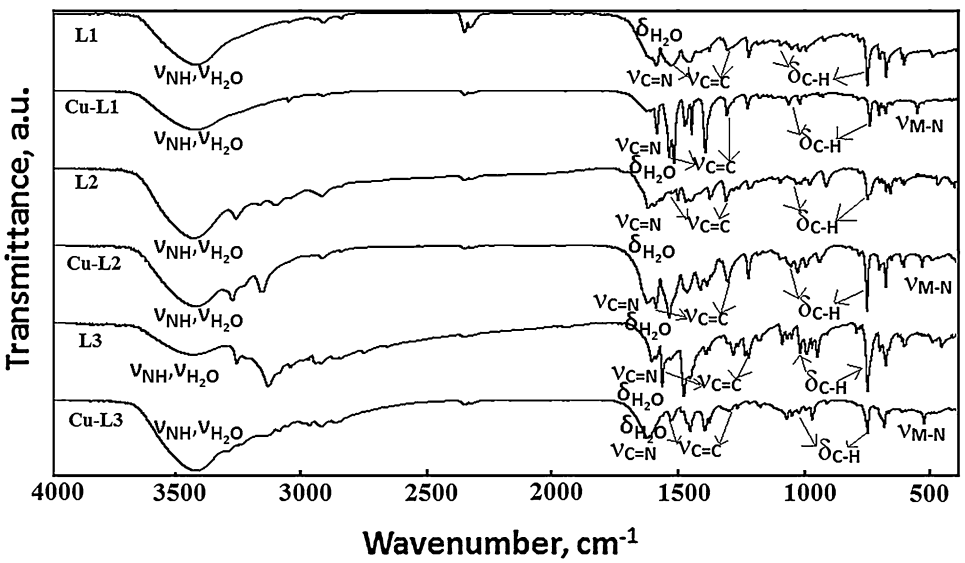

Fig. 1 FT-IR spectra of L1, L2, and L3 as well as their corresponding Cu(II) complexes, respectively

CH_3-Triazole-**L3**) and 2.65 (q, 4H, CH_2-Triazole-**L3**) [29]. The disappearances of NH in ^{1}H-NMR (d_6-DMSO-D2O) prove the presence of NH in the synthesized compounds.

3.2 Synthesis and Characterization of Cu(II) Triazole Schiff Base Complexes

Solid Cu(II)-triazole Schiff base complexes were synthesized via refluxing the mixture of the synthesized Schiff bases and copper chloride dihydrate in ethanol at 1:1 ratio in the presence of sodium acetate trihydrate. All the synthesized Cu(II) complexes are stable at room temperature, and soluble in DMSO and DMF. The synthesized complexes were characterized using different tools such as CHN elemental analyses, molar conductivity, FT-IR spectrum, magnetic moments, ESR, DTG analysis, and UV–Vis spectrophotometer. The Practical values of elemental analyses are in excellent agreement with the proposed molecular formulas (Theoretical values). The proposed structures of the complexes are shown in scheme 1. The molar conductivity measurements at 10^{-3} M in DMF prove that these copper complexes are nonelectrolytes.

3.2.1 FT-IR Spectra of Cu(II) Triazole Schiff Base Complexes

The FT-IR spectra of the synthesized triazole Schiff bases showed different bands; a medium intensity broad band appeared in the range 3500–3470 cm^{-1} is probably attributed to stretching NH vibration of the triazole ring and stretching vibration of the adsorbed water molecules [30]. This aforementioned band was appeared in all copper complexes (*c.f.* Fig. 1) in the range 3470–3455cm^{-1}, proving that NH is not contribute in coordination whereas a medium to high intensity band was observed in the range 1628–1620 cm^{-1} was assigned to C=N stretching vibration which decreased by 20–25 to 1607–1599 cm^{-1}. This proves triazole Schiff base coordination to copper through the nitrogen of C=N. Further supporting is achieved by the appearance of a medium intensity band in the region of 525–523 cm^{-1} which may be attributed to Cu-N stretching vibration [31]. The peak appeared at 1628–1620 cm^{-1} can also be attributed to bending vibrations of the adsorbed water molecules.

3.2.2 Electronic Spectra of Cu(II) Triazole Schiff Base Complexes

Octahedral crystal field environment is characterized by the ground state electronic configuration of Cu^{2+} is $t_{2g}{}^6e_g{}^3$ which produce $^2\mathbf{E_g}$ term whereas the excited state electronic configuration is $t_{2g}{}^5e_g{}^4$ which refers to $^2\mathbf{T_{2g}}$ term. Hence only one single electron transition, i.e., $^2\mathbf{E_g} \rightarrow {}^2\mathbf{T_{2g}}$, is available in an octahedral crystal field. The difference value is 10 Dq. The octahedral coordination is distorted either by compression or elongation of octahedron leading to tetragonal symmetry. It is noteworthy that, the ground $^2\mathbf{E_g}$ state is divided due to Jahn–Teller effect and hence lowering of symmetry is expected for Cu(II) ion. This state is divided into $^2\mathbf{B_{1g}}$ ($\mathbf{d_{x2-y2}}$) and $^2\mathbf{A_{1g}}$ ($\mathbf{d_{z2}}$) states in tetragonal symmetry and the excited term $^2\mathbf{T_{2g}}$ also is divided into $^2\mathbf{B_{2g}}$ ($\mathbf{d_{xy}}$) and $^2\mathbf{E_g}$ ($\mathbf{d_{xz}}$, $\mathbf{d_{yz}}$) levels. Electronic spectra of the synthesized Cu(II) complexes clearly show broad bands in the region 14,554–14,875 cm^{-1} with a shoulder on the low energy side at 11,220–11,882 cm^{-1}, which can be attributed to $^2\mathbf{B_{1g}} \rightarrow {}^2\mathbf{E_g}$ and $^2\mathbf{B_{1g}} \rightarrow {}^2\mathbf{A_{1g}}$ transition, respectively in a tetragonally distorted octahedral configuration as shown in Table 1 [9].

3.2.3 Magnetic Studies and Conductivity Measurements of Cu (II) Triazole Schiff Base Complexes

The magnetic moment measurements of the synthesized complexes: Cu(II)-**L1**, Cu(II)-**L2**, and Cu(II)-**L3**, are found to be 1.76, 1.84 and 1.77 B.M., respectively, which are considered slightly higher than 1.73 B.M (Spin only value of one unpaired electron) [9]. The molar conductivity values for Cu(II)-**L1**, Cu(II)-**L2**, and Cu(II)-**H3** complexes are 25.40, 27.60 and 26.20 Ω^{-1} cm^2 mol^{-1}, respectively, indicating the non-electrolyte nature of the prepared copper complexes [9].

3.2.4 ESR of Cu(II) Triazole Schiff Bases Complexes

Absorption of radiation of microwave frequency by molecules possessing unpaired spins electrons are described by electron spin resonance (ESR) spectroscopy [9]. This method is a vital tool for the analysis of the structure of ions or molecular systems containing unpaired electrons, which have spin-degenerate ground states in the absence of magnetic field. In the study of solid state compounds, ESR method is achieved to understand the symmetry of environments of the paramagnetic ion and the type of its bonding to the nearest neighboring ligands. When a paramagnetic material is placed in a magnetic field (H), the unpaired electron in the outer shell tends to align with the applied field. So the twofold spin degeneracy is finished. Thus the two energy levels, $\mathbf{E_{1/2}}$ and $\mathbf{E_{-1/2}}$ are separated by gap value equals to gβH value, where g is spectroscopic splitting factor and is called gyro magnetic ratio which divided into two types (g_{11} (in z-direction) and $g_\perp$ (in x or y-direction)) and β is the Bohr magneton. For a transition between these two energy levels, there is a finite probability. Hence, a change in the energy state can be stimulated by an external radio frequency. When microwave frequency ($\boldsymbol{\upsilon}$) is applied perpendicular to the direction of the applied magnetic field, resonance absorption will occur between the two split spin levels. The resonance condition is given by, $h\boldsymbol{\upsilon} = g\beta H$, where h is Planck's constant. ESR results give rise to a new parameter, G which is defined as:

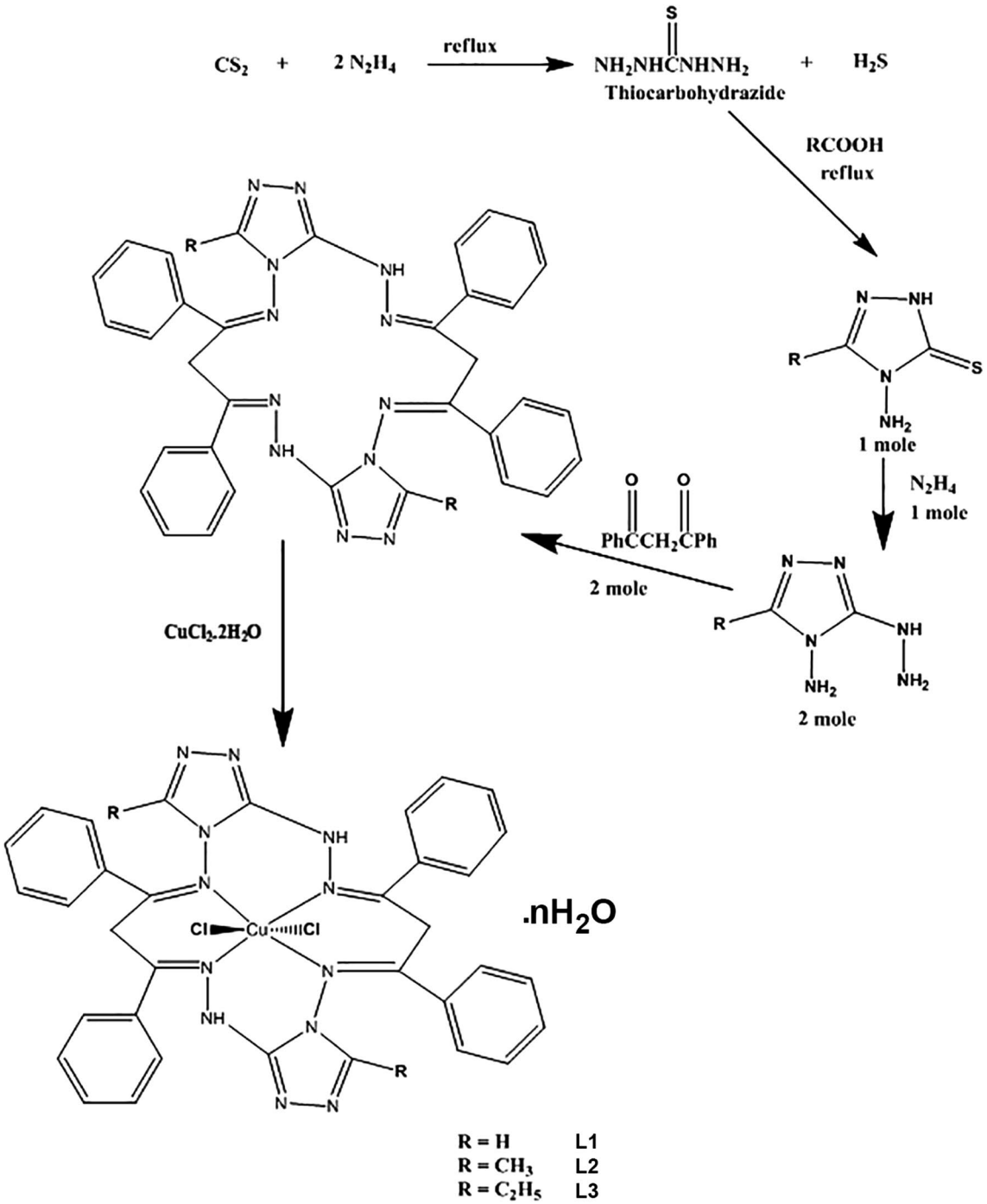

Scheme 1 Synthesis of 3-R-4-amino-5-hydrazino-1,2,4-triazole Schiff bases (L1, L2 and L3) and their Cu(II) complexes

$$G = \frac{(g_{11} - g_e)}{g_\perp - g_e}$$

where, g_e is the free electron g-value (2.0023).

The ESR spectrum of the synthesized Cu(II) complexes (*c.f.* Fig. 2) (Table 2) prove that $g_{11} > g_\perp > g_e$ (2.0023). Hence, this indicates an elongation tetragonal distortion where the unpaired electron is localized in the d_{x2-y2} orbital of Cu(II). It was found that the calculated G parameter observed for these copper complexes is <4 indicating exchange interactions in the solid copper complexes, in accordance with distorted octahedral configuration [9]. The optical absorption and ESR data in elongation tetragonal distortion are related as follows,

Table 1 Electronic absorption spectral data of the synthesized Cu(II) complexes

Complex	CT band		d → d bands		
	Nujol mull	DMF	Nujol mull	DMF	Assignment
Cu-L1	26891	28169	11220	11723	$^2B_{1g} \rightarrow {}^2A_{1g}$
			15367	14720	$^2B_{1g} \rightarrow {}^2E_g$
Cu-L2	30328	28328	11530	11884	$^2B_{1g} \rightarrow {}^2A_{1g}$
			14554	13678	$^2B_{1g} \rightarrow {}^2E_g$
Cu-L3	25954	28011	11882	11955	$^2B_{1g} \rightarrow {}^2A_{1g}$
			14875	15338	$^2B_{1g} \rightarrow {}^2E_g$

$$g_{11} = g_e - \frac{8\lambda}{\Delta E_{11(xy)}(^2B_1 \rightarrow {}^2B_2) = \Delta_{11}}$$

$$g_{\perp} = g_e - \frac{2\lambda}{\Delta E_{\perp(xy,yz)}(^2B_1 \rightarrow {}^2E) = \Delta_{\perp}}$$

Where λ is the spin–orbit coupling constant for free Cu(II) ion = −830 cm^{-1}. The calculated ΔE values are summarized in Table 2. Further, if A_{11}, g_{11} and $g_{\perp}$ values are known, α^2 (covalency parameter) can be estimated using the equation

$$\alpha^2 = (A_{II}/0.036) + (g_{II} - 2.0023) + 3/7(g\perp - 2.0023) + 0.04$$

3.2.5 *Thermogravimetric and Differential Thermal Analysis of Cu (II) Schiff Base Complexes*

TG and DTG curves (*c.f.* Fig. 3) for the synthesized Cu-**L3** Schiff base complex clearly showed five endothermic decomposition steps. The first step in the range 39–210 °C can be assigned to the loss of $3H_2O$ molecules with a weight loss of 6.5% (calc. 6.260%). The second step is probably

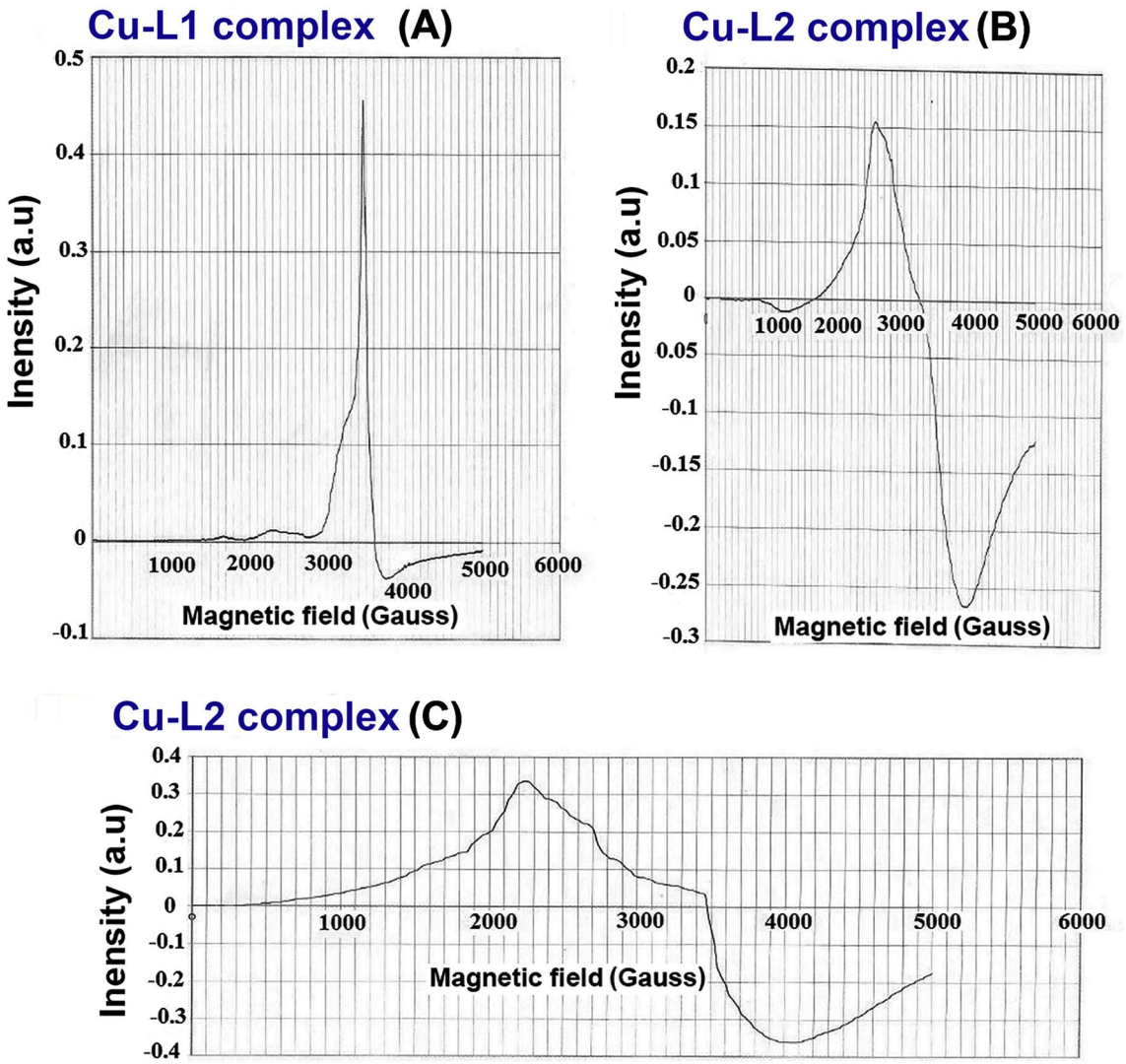

Fig. 2 ESR spectra of Cu-L1 (**a**), Cu-L2 (**b**), and Cu-L3 (**c**) complexes

Table 2 ESR spectral parameters of the synthesized Cu(II) complexes

Compound	g_{11}	$g_{\perp}$	G	α^2	ΔE	
					Δ_{II}	$\Delta_{\perp}$
Cu-L1	2.3	2.08	3.75	0.89	22133	20750
Cu-L2	2.9	2.3	3	–	7377	5533
Cu-L3	2.81	2.24	3.38	–	8197	6916

due to the loss of 2HCl molecules in the temperature range 210–225 °C with a weight loss of 8.3% (calc. 8.340%). The third step involved a weight loss of 25.3% (calc. 25.50%) in the temperature range of 225–300 °C which may be attributable to a loss of 2 $C_4N_4H_6$ organic moieties. The fourth step in the temperature range 300–470 °C can be assigned to loss of $C_{27}H_{30}N_2$ corresponding to a weight loss of 36.4% (calc. 36.17%). The last weight loss step in the temperature range of 470–670 °C can be assigned to the decomposition of the remaining organic part of the complex, 10.6% (calc. 10.78%), leaving CuO + 3 C residue with a percent of 12.9% (calc. 12.95%).

3.3 Synthesis and Characterization of Copper Oxide Nanoparticles

The synthesized solid complexes: Cu(II)-**L1**, Cu(II)-**L2** and Cu(II)-**L3**, were ignited at 650 °C to give the corresponding

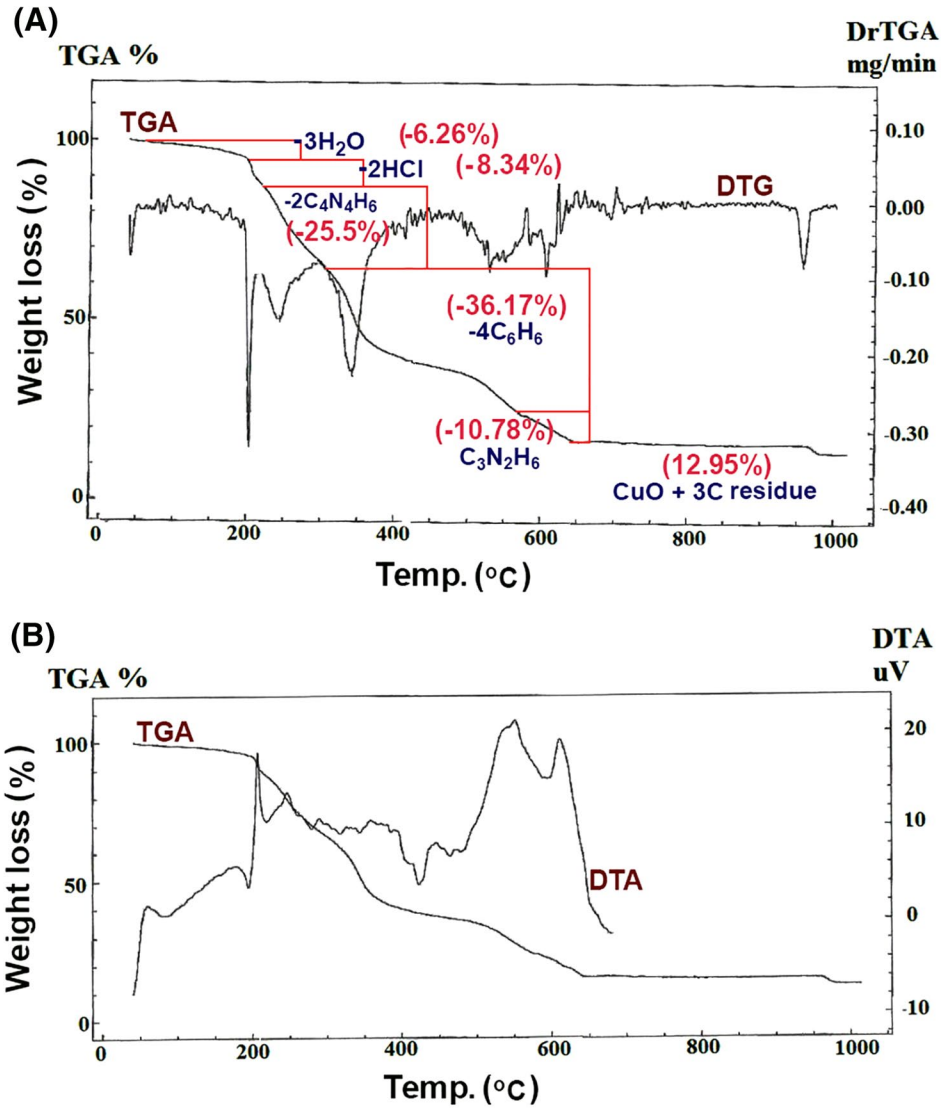

Fig. 3 Thermal analysis of Cu-L3 complex; TGA-DTG (**a**) and TGA-DTA (**b**)

copper oxide nanostructures, CuO. The produced copper oxide products were characterized using different tools such as XRD, FT-IR, HR-TEM, and UV–Vis spectrophotometer. Using this simple and fast chemical method, copper oxide nanoparticles can be prepared without using toxic solvents and expensive or complicated equipment.

3.3.1 XRD and HR-TEM of CuO Nanoparticles

The crystalline natures of the copper oxide nanoparticles were proved by using an X-ray diffractometer as clearly shown in Fig. 4. It was found from XRD patterns that all the characteristic peaks of copper oxide appeared in their positions without additional peaks due to impurities indicating the high purity of the prepared compounds. The results also showed that the prepared copper oxides belong to monoclinic system with cell constants: a = 4.678, b = 3.431 and c = 5.136 Å (space group C2/c, JCPDS card 80–0076) which are considered in excellent agreement with the ones published by H.M. Aly et al. [9]. The following Debye–Scherrer equation was used to calculate the average crystal size of the copper oxide nanoparticles [32–34]:

$$D = 0.9\lambda/\beta\cos\theta_B$$

Where, λ, β, Θ_B are the X-ray wavelength, the full width at half maximum (FWHM) of the diffraction peak and the Bragg diffraction angle, respectively. The calculated average crystallite size of copper oxide nanoparticles, obtained for **L1, L2** and **L3**, from XRD data, was found to be 24.50, 34.47 and 24.20 nm, respectively. Whereas, the HR-TEM images show the presence of sphere, cubic and irregular shapes particles with average particle size of 25.42, 35.35 and 28.75 nm, respectively as clearly shown in Fig. 4. Diffraction pattern from HR-TEM showed exactly the same d- spacing values (Ranging from 1.26 to 2.54 Å) obtained from XRD as shown in Fig. 4 which indicates the crystalline type of the synthesized copper oxide nanoparticles.

3.3.2 FT-IR of CuO Nanoparticles

The FT-IR spectra (*c.f.* Fig. 5) of the as-prepared copper oxide nanoparticles show the presence of many absorption peaks. The broad absorption bands appeared in the region 520–597 cm^{-1} can be attributed to Cu–O stretching vibration mode. The broad absorption band observed at 3450 cm^{-1} is assigned to the band O–H stretching vibrations whereas the weak band observed near 1640 cm^{-1} is assigned to H–O–H bending vibrations mode were also presented due to the adsorption of water in air when FT-IR sample disks were carried in an open air [9, 35, 36].

3.3.3 Optical Properties of CuO Nanoparticles

In order to examine the semiconductor properties of the prepared copper oxide nanoparticles, UV–Vis absorption spectra were performed as clearly shown in Fig. 5. The optical band energy gap E_g was calculated using the following equation: $(\alpha h\upsilon)^n = K(h\upsilon - Eg)$ where α is the absorption coefficient, K is a constant, E_g is the optical band energy gap and n equals either two for an direct allowed transition or 1/2 for an indirect allowed transition. In case of the prepared copper oxides, hυ (eV) is plotted versus $(\alpha h\upsilon)^2$, as clarified in Fig. 5. The extrapolation of each graph to zero value of $(\alpha h\upsilon)^2$ gives the direct optical band gap (E_g) which is found to be 0.96, 1.00, and 0.87 eV for copper oxide nanoparticles obtained from **L1, L2** and **L3**, respectively. These energy gap values prove that the as-prepared copper oxide nanoparticles products have semiconductors properties [9].

4 Biological Activities

The in-vitro biological activity of all the synthesized Schiff bases (**L1, L2** and **L3**), their Cu (II) complexes, and as-prepared copper oxides were studied using bacteria, *Staphylococcus aureus* and *Escherichia coli* and fungi, *Candida albicans* and *Aspergillus flavus*. In the antimicrobial studies ampicillin was chosen as antibacterial agent whereas, amphotericin b was chosen as antifungal agent and the two worked together as positive control. Negative control of antimicrobial studies achieved through filter disc impregnated with 10 µL of solvent (DMSO). The tested compounds diffuse from the disc into the agar; only around the disc during the time of incubation. When the organism is exposed to the compounds, it will not grow in an area around the disc called "zone of inhibition", which measured and clarified in Table 3. The Schiff base **L3** compound showed very strong activity against all pathogens (both bacteria and fungi). All the synthesized compounds showed poor antifungal activity and moderate activity against both pathogenic bacteria strains. It was found also that all copper oxides, showed no activity on both of *C. albicans* and *A. flavus* fungi.

5 Application of CuO Nanoparticles in Photocatalytic Degradation of Methylene Blue Dye

The degradation of methylene blue dye has been studied in the presence of copper oxide catalyst (prepared from Cu-L3 complex) under ultraviolet radiation, in the presence of hydrogen peroxide via photo Fenton reaction [9]. This copper oxide sample has been chosen because of its high surface area and low crystal size (24.20 nm). The UV–Vis

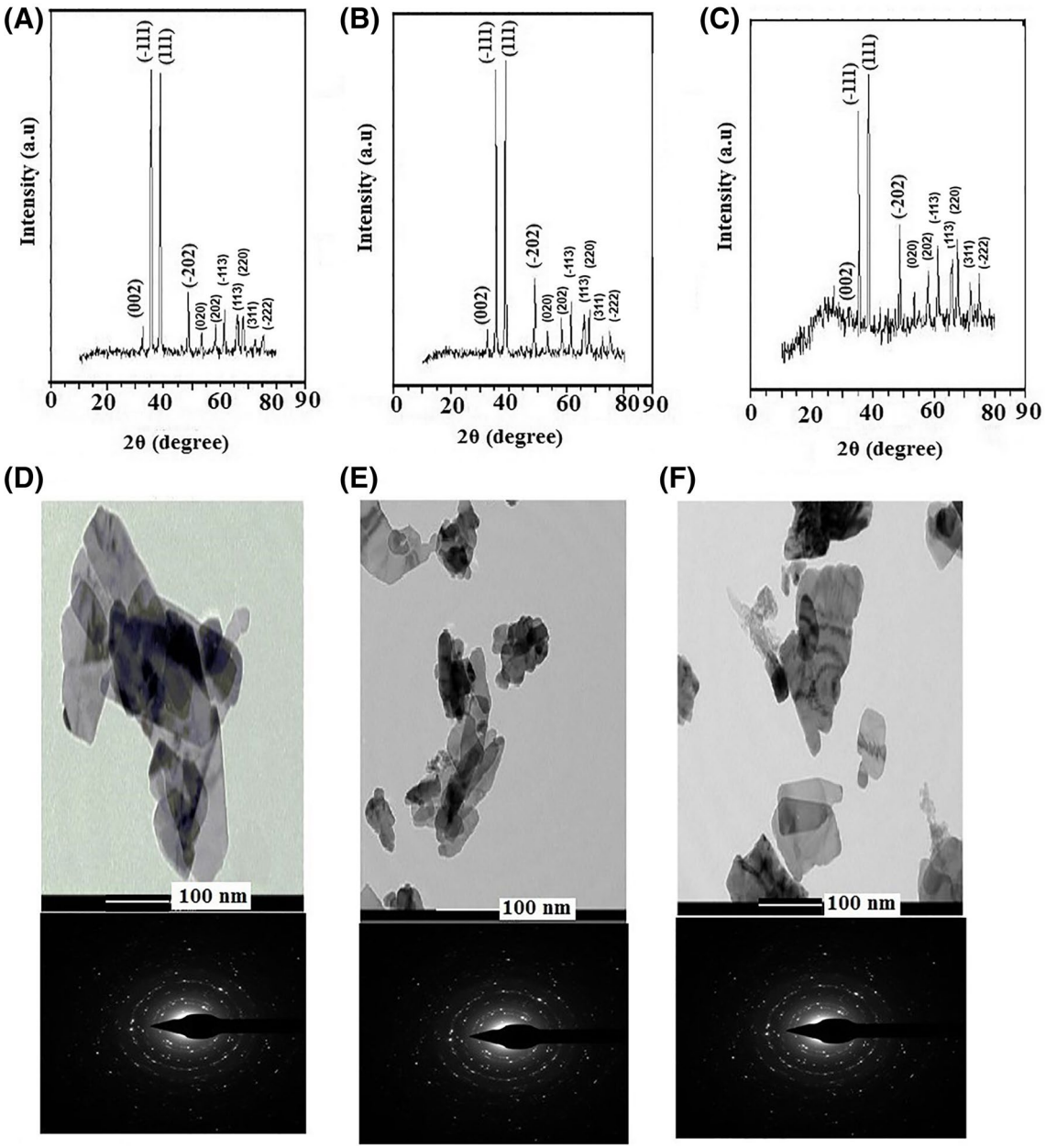

Fig. 4 XRD patterns of CuO nanoparticles prepared from copper complexes of L1 (**a**), L2 (**b**), and L3 (**c**) as well as the corresponding HR-TEM images, respectively

spectra of degraded dye at different times from zero up to 8 h in the presence of copper oxide catalyst and hydrogen peroxide has been illustrated in Fig. 6a, b. It was found that the degradation percent of dye increased with time until amounted to about 77.36% after 360 min, which was considered a high percent compared with what exists in the literatures [9]. Numerous experiments to degrade the dye in the presence or absence of ultraviolet radiation have been carried out but it was not greatly effective (Figures omitted for brevity). Photodegradation reaction mechanism in the presence of UV only, (CuO Catalyst + UV) and (UV + CuO Catalyst + H_2O_2) has been clarified in Scheme 2.

In case of UV only, the interaction between methylene blue dye and ultraviolet radiation produces excited dye molecule which reacts with oxygen to generate positive radical cation of dye ($MB^{+\cdot}$) and negative radical anion of oxygen ($O_2^{-\cdot}$). After that negative radical anion reacts with H^+ (liberated from water) generating super oxide radical ($OOH^{\cdot}$) which characterized by high power of degradation toward dye molecules.

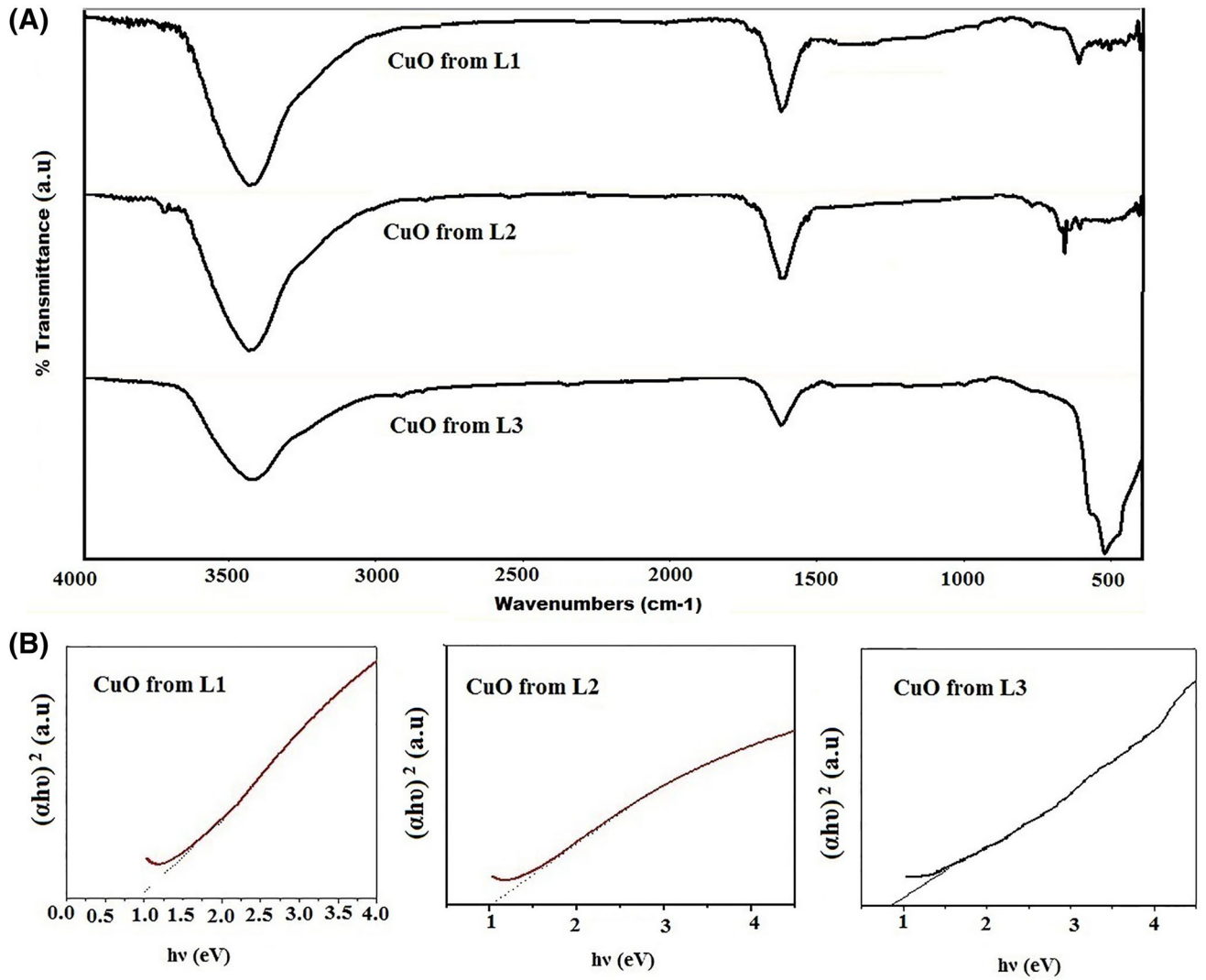

Fig. 5 FT-IR spectra CuO nanoparticles prepared from copper complexes of L1 (**a**), L2 (**b**), and L3 (C) as well as the corresponding optical gap energies, respectively

Table 3 The antimicrobial activity (in-vitro) of the synthesized triazole Schiff bases, their Cu (II) complexes and their copper oxide nanoparticles

Compound	Bacteria		Fungi	
	E. coli (G^-)	*S. aureus* (G^+)	*A. flavus*	*C. albicans*
L1	11	11	9	9
L2	11	11	9	9
L3	30	31	26	9
Cu-L1	9	9	0	0
Cu-L2	10	10	0	10
Cu-L3	11	10	0	0
CuO From L1	10	11	0	0
CuO From L2	10	11	0	0
CuO From L3	10	11	0	0

In case of UV + CuO catalyst, the interaction between copper oxide and ultraviolet radiation produces holes (h^+) and electrons (e^-) on the surface of catalyst. The produced electrons on oxide react with oxygen to generate negative radical anion of oxygen ($O_2^{-\cdot}$) which reacts with water to produce superoxide radical ($OOH^{\cdot}$). On the other hand, holes of the oxide react with both water and hydroxide anion to generate hydroxide radicals ($OH^{\cdot}$). Both superoxide radical and hydroxide radicals effectively increase the rate of degradation of dye molecules. Addition of hydrogen peroxide in presence of copper oxide catalyst and UV light generate large amount of hydroxide radical ($OH^{\cdot}$) besides both of superoxide radical ($OOH^{\cdot}$) leading to very high degradation rate.

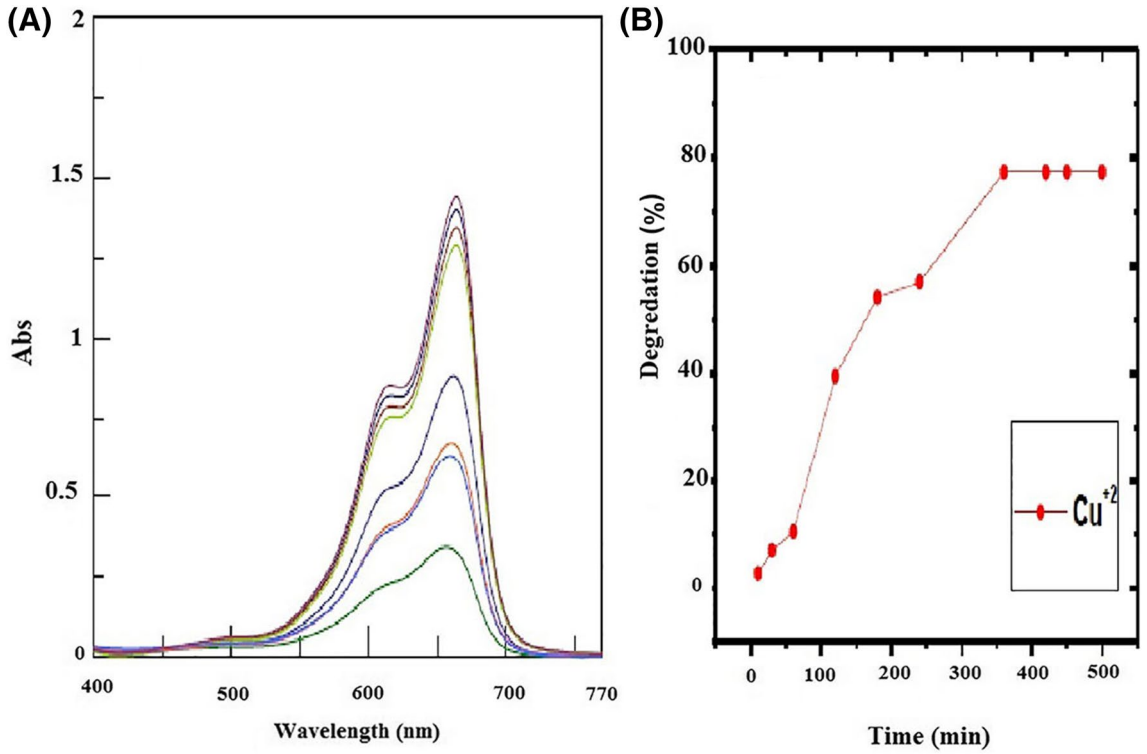

Fig. 6 photocatalytic degradation of methylene blue dye using CuO generated from Cu-L3 complex; absorbance of the remaining dye (**a**), and % degradation versus time (**b**)

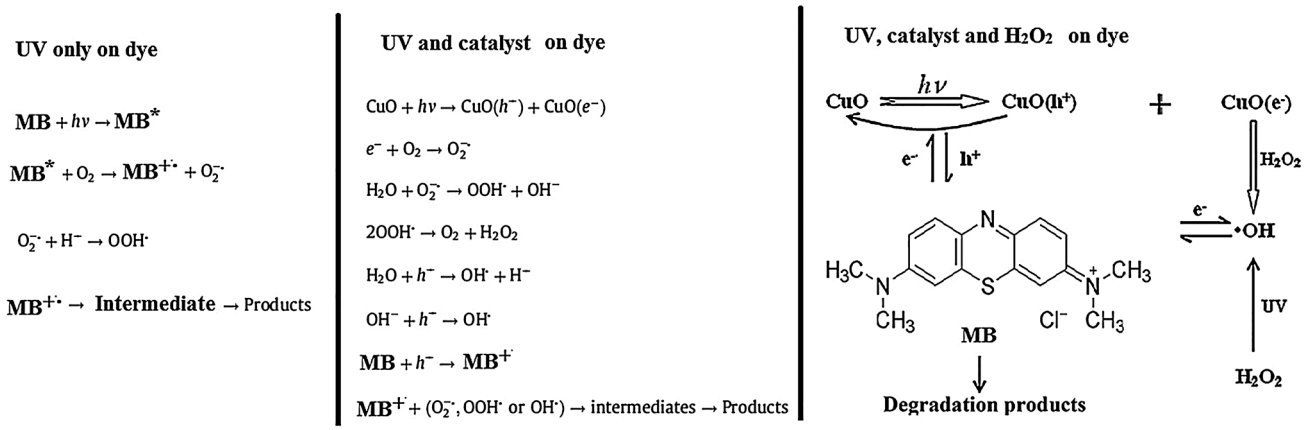

Scheme 2 Proposed reactions of the photodegradation of MB dye in the presence of UV only, catalyst + UV, and catalyst + H_2O_2 + UV

6 Conclusion

Three new Schiff base compounds were successfully synthesized via condensation of 3-R-4-amino-5-hydrazino-1,2,4-triazole with dibenzoylmethane [R = H, CH_3, and CH_2CH_3 namely L1, L2, and L3, respectively]. The corresponding Cu(II) complexes were synthesized via refluxing of Schiff bases with $CuCl_2.2H_2O$. All the synthesized copper complexes are nonelectrolytes in *N,N*-dimethylformamide (DMF). In addition to CuO nanoparticles have been produced from the thermal decomposition of the synthesized triazole Schiff base- copper complexes. The produced CuO nanoparticles were examined for the photocatalytic degradation of methylene blue dye in the presence of hydrogen peroxide under UV illumination. The results revealed that *ca*. 77.36% of the methylene blue dye was degraded within 6 h. All Schiff bases, their Cu(II) complexes, and CuO nanoparticles showed a moderate

activity against both pathogenic bacteria strains (*Staphylococcus aureus* & *Escherichia coli*) and poor antifungal activity (*Candida albicans* & *Aspergillus flavus*).

References

1. R. Shukla, T.P. Mohan, B. Vishalakshi, D. Chopra, Synthesis, crystal structure and theoretical analysis of intermolecular interactions in two biologically active derivatives of 1,2,4-triazoles. J. Mol. Struct. **1134** 426–434 (2017)
2. A.E.-B.A.G. Ghattas, H.M. Moustafa, E.A.A. Hassanein, B.R.M. Hussein, Synthesis and antibacterial activity of some new 4-anilino-5-phenyl-4H-1,2,4-triazole-3-thiol derivatives. Arab. J. Chem. **9**, S1654–S1659 (2016)
3. Z. Song, Y. Liu, Z. Dai, W. Liu, K. Zhao, T. Zhang, Y. Hu, X. Zhang, Y. Dai, Synthesis and aromatase inhibitory evaluation of 4-N-nitrophenyl substituted amino-4H-1,2,4-triazole derivatives. Bioorg. Med. Chem. **24**, 4723–4730 (2016)
4. N. Kulabas, E. Tatar, O. Bingol Ozakpinar, D. Ozsavci, C. Pannecouque, E. De Clercq, I. Kucukguzel, Synthesis and antiproliferative evaluation of novel 2-(4H-1,2,4-triazole-3-ylthio)acetamide derivatives as inducers of apoptosis in cancer cells. Eur. J. Med. Chem. **121**, 58–70 (2016)
5. K. Wajda-Hermanowicz, D. Pieniążczak, R. Wróbel, A. Zatajska, Z. Ciunik, S. Berski, A study on the condensation reaction of aryl substituted 4-amine-1,2,4-triazole with benzaldehydes: structures and spectroscopic properties of schiff bases and stable hemiaminals. J. Mol. Struct. **1114**, 108–122 (2016)
6. R. Alphonse, A. Varghese, L. George, Synthesis, characterization and photophysical studies of a novel schiff base bearing 1, 2, 4-Triazole scaffold. J. Mol. Struct. **1113**, 60–69 (2016)
7. B.N. Prasanna Kumar, K.N. Mohana, L. Mallesha, Synthesis and antiproliferative activity of some new fluorinated Schiff bases derived from 1,2,4-triazoles. J. Fluorine. Chem. **156**, 15–20 (2013)
8. H. Khanmohammadi, M. Erfantalab, G. Azimi, New acyclic 1,2,4-triazole-based Schiff base hydrazone: synthesis, characterization, spectrophotometric and computational studies. Spectrochim. Acta. A **105**, 338–343 (2013)
9. H.M. Aly, M.E. Moustafa, M.Y. Nassar, E.A. Abdelrahman, Synthesis and characterization of novel Cu(II) complexes with 3-substituted-4-amino-5-mercapto-1,2,4-triazole Schiff bases: a new route to CuO nanoparticles. J. Mol. Struct. **1086**, 223–231 (2015)
10. M. Iranifam, N.R. Hendekhale, CuO nanoparticles-catalyzed hydrogen peroxide–sodium hydrogen carbonate chemiluminescence system used for quenchometric determination of atorvastatin, rivastigmine and topiramate. Sens. Actuators. B. Chem. **243**, 532–541 (2017)
11. M. Maruthupandy, Y. Zuo, J.-S. Chen, J.-M. Song, H.-L. Niu, C.-J. Mao, S.-Y. Zhang, Y.-H. Shen, Synthesis of metal oxide nanoparticles (CuO and ZnO NPs) via biological template and their optical sensor applications. Appl. Sur. Sci. **397**, 167–174 (2017)
12. P. Liu, X. Xia, W. Lei, Q. Hao, Rational synthesis of highly uniform hollow core–shell Mn_3O_4/CuO@TiO_2 submicroboxes for enhanced lithium storage performance. Chem. Eng. J. **316**, 214–224 (2017)
13. A. Ajmal, I. Majeed, R.N. Malik, M. Iqbal, M.A. Nadeem, I. Hussain, S. Yousaf, G. Zeshan, Mustafa, M.I. Zafar, M.A. Nadeem, Photocatalytic degradation of textile dyes on Cu_2O-CuO/TiO_2 anatase powders. J. Environ. Chem. Eng. **4**, 2138–2146 (2016)
14. A. Taufik, R. Saleh, Synthesis of iron(II, III) oxide/zinc oxide/copper(II) oxide (Fe_3O_4/ZnO/CuO) nanocomposites and their photosonocatalytic property for organic dye removal. J. Colloid. Interface. Sci. **491**, 27–36 (2017)
15. H. Xie, L. Zhu, W. Zheng, J. Zhang, F. Gao, Y. Wang, Microwave-assisted template-free synthesis of butterfly-like CuO through $Cu_2Cl(OH)_3$ precursor and the electrochemical sensing property. Solid. State. Sci. **61**, 146–154 (2016)
16. S. Sonia, R. Jayasudha, N.D. Jayram, P.S. Kumar, D. Mangalaraj, S.R. Prabagaran, Synthesis of hierarchical CuO nanostructures: biocompatible antibacterial agents for Gram-positive and Gram-negative bacteria. Curr. Appl. Phys. **16**, 914–921 (2016)
17. C. Dong, X. Xing, N. Chen, X. Liu, Y. Wang, Biomorphic synthesis of hollow CuO fibers for low-ppm-level n-propanol detection via a facile solution combustion method. Sens. Actuators. B. Chem. **230**, 1–8 (2016)
18. X. Liu, G. Liu, L. Wang, Y. Li, Y. Ma, J. Ma, Morphology- and facet-controlled synthesis of CuO micro/nanomaterials and analysis of their lithium ion storage properties. J. Power. Sources **312**, 199–206 (2016)
19. G.B. Bagihalli, S.A. Patil, Synthesis, spectral characterization, in vitrobiological and DNA cleavage studies of Co(II), Ni(II), Cu(II), and Zn(II) complexes with 1,2,4-triazole Schiff bases. J. Coord. Chem. **62**, 1690–1700 (2009)
20. B. Shivarama Holla, B. Veerendra, M.K. Shivananda, B. Poojary, Synthesis characterization and anticancer activity studies on some Mannich bases derived from 1,2,4-triazoles. Eur. J. Med. Chem. **38**, 759–767 (2003)
21. M.Y. Nassar, E.I. Ali, E.S. Zakaria, Tunable auto-combustion preparation of TiO_2 nanostructures as efficient adsorbents for the removal of an anionic textile dye. RSC Adv. **7**(13), 8034–8050 (2017)
22. M.Y. Nassar, T.Y. Mohamed, I.S. Ahmed, I. Samir, MgO nanostructure via a sol-gel combustion synthesis method using different fuels: an efficient nano-adsorbent for the removal of some anionic textile dyes. J. Mol. Liq. **225**, 730–740 (2017)
23. M.Y. Nassar, M.M. Moustafa, M.M. Taha, Hydrothermal tuning of the morphology and particle size of hydrozincite nanoparticles using different counterions to produce nanosized ZnO as an efficient adsorbent for textile dye removal. RSC Adv. **6**(48), 42180–42195 (2016)
24. M.Y. Nassar, S. Abdallah, Facile controllable hydrothermal route for porous $CoMn_2O_4$ nanostructure: synthesis, characterization, and textile dye removal from aqueous media. RSC Adv. **6**(87), 84050–84067 (2016)
25. M.Y. Nassar, M. Khatab, Cobalt ferrite nanoparticles via a template-free hydrothermal route as an efficient nano-adsorbent for potential textile dye removal. RSC Adv. **6**(83), 79688–79705 (2016)
26. M.Y. Nassar, I.S. Ahmed, I. Samir, A novel synthetic route for magnesium aluminate ($MgAl_2O_4$) nanoparticles using sol–gel auto combustion method and their photocatalytic properties. Spectrochim. Acta Part A **131**, 329–334 (2014)
27. M. Mostafa, H.M. Saber, A.A. El-Sadek, M.Y. Nassar, Preparation and performance of $^{99}Mo/^{99m}Tc$ chromatographic column generator based on zirconium molybdosilicate. Radiochim. Acta **104**, 257–265 (2016)
28. A.K. Singh, O.P. Pandey, S.K. Sengupta, Synthesis, spectral characterization and biological activity of zinc(II) complexes with 3-substituted phenyl-4-amino-5-hydrazino-1, 2, 4-triazole Schiff bases. Spectrochim. Acta. Part A **85**, 1–6 (2012)
29. G.B. Bagihalli, P.G. Avaji, S.A. Patil, P.S. Badami, Synthesis, spectral characterization, in vitro antibacterial, antifungal and cytotoxic activities of Co(II), Ni(II) and Cu(II) complexes with 1,2,4-triazole Schiff bases. Eur. J. Med. Chem. **43**, 2639–2649 (2008)

30. M.Y. Nassar, A.S. Attia, K.A. Alfallous, M.F. El-Shahat, Synthesis of two novel dinuclearmolybdenum(0) complexes of quinoxaline-2,3-dione: new precursors for preparation of α-MoO_3 nanoplates. Inorg. Chim. Acta **405**, 362–367 (2013)
31. M.Y. Nassar, I.S. Ahmed, Hydrothermal synthesis of cobalt carbonates using different counter ions: an efficient precursor to nano-sized cobalt oxide (Co_3O_4). Polyhedron **30**, 2431–2437 (2011)
32. M.Y. Nassar, I.S. Ahmed, Template-free hydrothermal derived cobalt oxide nanopowders: synthesis, characterization, and removal of organic dyes. Mater. Res. Bull. **47**, 2638–2645 (2012)
33. M.Y. Nassar, Size-controlled synthesis of $CoCO_3$ and Co_3O_4 nanoparticles by free-surfactant hydrothermal method. Mater. Lett. **94**, 112–115 (2013)
34. M.Y. Nassar, T.Y. Mohamed, I.S. Ahmed, One-pot solvothermal synthesis of novel cobalt salicylaldimine–urea complexes: a new approach to Co_3O_4 nanoparticles. J. Mol. Struct. **1050**, 81–87 (2013)
35. M.Y. Nassar, A.S. Amin, I.S. Ahmed, S. Abdallah, Sphere-like Mn_2O_3 nanoparticles: facile hydrothermal synthesis and adsorption properties., J. Taiwan Inst. Chem. Eng. **64** 79–88 (2016)
36. M.Y. Nassar, I.S. Ahmed, T.Y. Mohamed, M. Khatab, A controlled, template-free, and hydrothermal synthesis route to sphere-like α-Fe_2O_3 nanostructures for textile dye removal. Rsc. Adv. **6**, 20001–20013 (2016)